Sustainable Materials and Technologies 41 (2024) e01119

Contents lists available at ScienceDirect

Sustainable Materials and Technologies

journal homepage: www.elsevier.com/locate/susmat

Life cycle assessment of limestone calcined clay concrete: Potential for low-carbon 3D printing

Willy Jin [a,b,*], Charlotte Roux [c], Claudiane Ouellet-Plamondon [b], Jean-François Caron [a]

[a] Navier Laboratory, École des Ponts ParisTech, Gustave Eiffel University, CNRS, Champ-Sur-Marne, France
[b] Department of Construction Engineering, École de Technologie Supérieure, Montreal, Quebec, Canada
[c] École des Mines de Paris, PSL University, Paris, France

A R T I C L E I N F O

Keywords:
Limestone calcined clay blend
Life cycle assessment
3D printing

A B S T R A C T

Limestone calcined clay cement is being promoted throughout the construction industry as a way to considerably reduce the cement proportion in concrete mixtures. At the same time, concrete 3D printing could save resources by placing concrete material only where its functionalities are maximized. This study addresses the need for a quantification of the environmental impacts related to the material acquisition phase regarding a low-clinker 3D printing material.

Compared to a 30 MPa 3D printing material from the literature, a 3D printable LC3-based concrete with low clinker content in the Quebec context displays a 36 % climate change score reduction with the same compressive strength (46 % reduction in the French context). A small impact shift is noticed in 6 out of 16 midpoint indicators (5 in the French case), mainly due to the calcined clay production. However, it is offset by the significant reduction in other indicators when considering an endpoint assessment. When considering different sourcing scenarios, a global warming potential variability of up to 15 % is observed.

LC3 remains a viable solution for the mitigation of greenhouse gas emissions in the context of concrete 3D printing as it provides mechanical strength and enhanced structuration rate for low-clinker materials. However, a specific attention should be accorded to the calcined clay plant locations, especially when the calcined clay content is higher than the value used in this study. As a perspective, a mix design tool could allow the optimization of environmental impacts depending on expected fresh and hardened properties.

1. Introduction

Additive manufacturing in the construction industry is already allowing to manufacture structures from prototypes to production units [1]. The added value of this technology relies on multiple benefits ranging from the architectural freedom it provides to the industrialization potential for a rise in productivity along with the reduction in physical labour [2,3]. Crucially, it also proposes a reduction of environmental impacts justified by the material use reduction originating from structural optimization and the absence of formwork [4]. In that regard, the adoption of digital fabrication could justify a reduction in greenhouse gas emissions between 37 % [5] and 50 % [6], depending on the structure complexity.

In the construction industry, in which the global production of cement represents 8 % of global greenhouse gas emissions [7], solutions for an increase in productivity along with a decrease in environmental impacts are essential to meeting the demand while complying with planetary boundaries [8]. In this regard, the quantification of the environmental impacts for the whole value chain - material acquisition, structure design, shaping process, use phase, end of life - of both conventional and innovative construction methods are necessary in order to evaluate the best scenario for each application. With this perspective, a life cycle assessment (LCA) of a 3D printing process has been carried out [9]. Several studies have pointed out the potential impact mitigation emerging from the expanded design opportunities [10,11]. Eventually, the material production is one of the most determining levers for reducing environmental impacts [12,13]. As such, the quantification of these impacts through contextualized life cycle assessment is essential.

The collected values of global warming potential (GWP) for conventional and 3D printable (3DP) concretes show different trends. For conventional construction, the variability is relatively low and the climate change score of 30 to 60 MPa concretes (C30, C60) span around the 300 kg CO_2-eq/m^3 mark [5,6,12,14]. This is confirmed in the

* Corresponding author at: Navier Laboratory, École des Ponts ParisTech, Gustave Eiffel University, CNRS, Champ-Sur-Marne, France.
E-mail address: zibo.jin@enpc.fr (W. Jin).

https://doi.org/10.1016/j.susmat.2024.e01119
Received 13 June 2024; Received in revised form 9 August 2024; Accepted 11 September 2024
Available online 19 September 2024

Nomenclature

3DPM	3D printing material
1 K	1 component system
2 K	2 component system
OPC	Ordinary Portland cement
LC3	Limestone calcined clay cement
SCM	Supplementary cementitious materials
LCA	Life cycle assessment
LCIA	Life cycle impact assessment
EI	Ecoinvent 3.7 Cutoff
GHG	Greenhouse gas
GWP	Global warming potential
ClCh	Climate change
CA	Canada
QC	Quebec
SK	Saskatchewan
GLO	Global
RER	Rest of Europe
RoW	Rest of world
GUbSF	General use (Portland cement) blended with silica fume
CC	Calcined clay
LF	Limestone filler
W	Water
Sa	Sand
PCE SP	Polycarboxylate ether superplasticiser
LC3 QC	LCA model of LC3 reference blend (30 MPa) in the Quebec context
LC3 FR	LCA model of LC3 (30 MPa) contextualized to France
OPC QC	LCA model of literature 3D printing mortar (30 MPa) contextualized to Quebec
OPC FR	LCA model of literature 3D printing mortar (30 MPa) contextualized to France

Quebec context by the Environmental Product Declaration of *Association Béton Quebec* for industry-wide ready-mix concrete which estimates the climate change score of 30 MPa interior concrete without air-entraining admixture at 311 kg CO_2-eq/m^3 [15].

In the specific context of 3D printing, conflicting rheological requirements must be fulfilled in the same time frame [16] in the case of 2 K 3D printing materials (3DPM), which rely on the secondary mixing of a chemical accelerator before extrusion, and especially for 1 K 3DPM, which include no acceleration. Higher cement content reduces internal friction, providing better shearing ability [17], but also enhances both the attractive colloidal forces for the initial yield stress and the nucleation of hydrates for the continuous increase of elastic modulus [18]. Thus, the majority of 3D printing materials are mortars with high cement content in the binder (> 60 % [19]) and high paste proportion in the mortar (400 to 700 kg/m^3 [20]). As clinker is the main contributor to climate change score in concrete [21], this score is typically 30 % higher for 3DPM compared to conventional concretes [4,5,12]. In this context, the material savings enabled by 3D printing must be concurrent with a mitigation of material unit volume impact, meaning a decrease of cement content.

Supplementary cementitious materials (SCM) have been widely used in the construction industry [22,23], replacing up to 45 % of the cement in conventional concretes but this substitution rate is unusual in the 3D printing industry. Pozzolanic and hydraulic co-products from coal, steel or silicon alloy industries (fly ash, ground granulated blast furnace slag, silica fume) are available in limited proportions when compared to the production of clinker and are compelled to decrease in the coming years [24]. In this context, the ternary limestone calcined clay cement (LC3) utilizes the synergy between calcined clay, calcium carbonate and cement in order to yield concretes with up to 50 % cement substitution and comparable mechanical properties [25]. The additional hydrates in LC3 help maintain these properties by filling the porosity and contributing to the hardened microstructural network [26]. Additionally, these hydrates benefit durability properties such as resistivity or chloride penetration resistance [27]. The structuration rate of LC3 is higher than Portland cement (OPC) considering the calcined clay higher water demand and its finer granulometry [28]. Besides, its higher static yield stress, plastic viscosity and cohesiveness [29] justify the application of LC3 to 3D printing with a potential reduction of environmental impacts. Indeed, studies indicate a suitable rheological behavior at fresh state considering the higher reactivity of alumina in the metakaolin, coupled with its higher specific surface and layered structure [30–32]. Several studies [33,34] suggest that a substitution of 75 % is possible while maintaining a compressive strength of 30 MPa and the printability potential of LC3 has been confirmed [33,35,65]. Additionally, accelerated carbonation and carbon sequestration for LC3 materials could complement this path to low-carbon concretes [36,37]. Consequently, there stands a potential for an optimized 3DPM with high cement substitution and adjustable strength for specific applications. In order to achieve this, a thorough definition of printability needs to be established for 1 K 3D printing.

Concerning the global warming potential of LC3, studies report a reduction in greenhouse gas (GHG) emissions of 30 to 50 % compared to conventional Portland concrete [38,39]. To the author's knowledge, only one study for 3D printable LC3 [32] states a 50 % reduction in GHG emissions compared to a Portland cement 3DPM, but considers only uncontextualized raw material impacts. When considering other impact categories, the number of studies on 3DPM is very limited. When comparing conventional construction and concrete 3D printing, Han et al. [12] state that, in the material acquisition phase for acidification and eutrophication, the scores are generally higher (respectively 21.6 % and 11.3 %) for the second construction technique. On the contrary, the 3DPM performs 7.3 % better in the photochemical pollution category. These mean values are considered for several Portland cement-based mixtures including more or less recycled aggregates. Alhumayani et al. [20] present a contribution analysis for a 3D printed 1 m^2 wall. A sensitivity analysis carried out on several 3DP materials from the literature indicates a contribution of cement and fly ash of around 90 % of overall impacts, including ozone depletion, fine particulate matter formation, marine eutrophication, land use or mineral resource scarcity. In regards to LC3 for conventional construction, Huang et al. [40] observe an increased score in the ozone depletion potential, the freshwater ecotoxicity potential, freshwater eutrophication potential and marine eutrophication potential, mainly due to calcined clay production. In the other categories, the LC3 performs similarly or better compared to a standard concrete. Overall, studies have compared conventional and 3DP methods with OPC-based materials or tackled conventional LC3 materials. However, no study addresses a complete range of life cycle assessment methods for a low-clinker 3D printing LC3.

In the end, the construction industry must decrease its environmental impacts by reducing the volume of material consumed, but also by minimizing the impact of the materials that are effectively used. The synergy of calcined clay, limestone and cement enables a partial decoupling between cement content and mechanical properties or structuration rate, making LC3 promising for low-carbon 3D printing. However, to support this claim, a contextualized assessment of a comprehensive set of environmental indicators in the material acquisition phase is required for an 3D printable LC3-based concrete.

To address this research gap, this study proposes an original framework for the definition of printability applied to continuous mixing 1 K materials. Then, by developing a generic open-source LCA model and applying it to two novel use cases with distinct supply chain settings and grounded hypotheses, this study displays the main considerations of environmental impacts and process contributions of LC3 components. Furthermore, an evaluation of impacts over an exhaustive set of indicators highlights the effects of calcined clay addition and the potential impact shifting is assessed via endpoint indicators evaluation. The opportunity that LC3 represents in the 3D printing industry is substantiated by a perspective on the influence of calcined clay production. Eventually, this study addresses all those aspects while setting the groundwork for a subsequent optimization methodology based on [41]. This mix design process could fully integrate the GWP in order to yield a printable LC3 mortar with minimized climate change score.

In the section 2 of this paper, the materials, characterization methods and analysis methodology are detailed. The functional unit is defined through lab-scale physical measurements and large-scale experiments with a 3D printing setup. The results are presented in the section 3 for the reference material. The interrogations, sensitivity analysis and limitations are discussed in the section 4.

2. Materials and methods

The objectives and general framework are detailed in the section 2.1 and the materials used are introduced in the section 2.2. The section 2.3 describes the experimental setup related to printability, namely flowability, shape retention and buildability at fresh state, along with the mechanical test performed on hardened samples. Additionally, the LCA main hypotheses are detailed. More information about the characterization methods can be found in the supporting information.

2.1. Definition of objectives and framework

The purpose of this study is to assess the potential of an LC3-based 3DPM towards mitigating the environmental impact of the concrete 3D printing industry. This investigation is divided in six steps detailed in the Table 1. The first three steps consist in setting up an LCA model, the next ones cover the research gaps identified in the introduction, namely the relevance of LC3 for low-carbon 3D printing in Quebec and France, especially considering various impact categories. The contextualization of our LCA model to two contrasting production and distribution scenarios (CA-QC and FR) constitutes a necessary analysis when progressing towards the use of more locally sourced raw materials on a global scale.

A comprehensive description of the printability requirements (step 1) as well as the trial and error process resulting in the reference mortar (step 2) is available in the supporting information. This includes the definition of rheological criteria at fresh state and correlation with large scale 3D printing. The scope of the study, the components of the life cycle inventory and the considerations of the functional unit are represented on Fig. 1.

Table 1
General study outline.

Step	Description
Step 1	Definition of a printable material relative to available printing setup: Selection of characterization protocol and specification of printability thresholds
Step 2	Material Mix Design: Low-clinker driven trial-and-error process resulting in reference LC3 mortar
Step 3	Constitution of Generic LC3 LCA Model: Identification of contextualizable processes
Step 4	Evaluation of GWP: Comparisons between literature OPC-based model and contextualized LC3 models in CA-QC and FR
Step 5	Analysis of Impact Shift: Assessment of comprehensive LCIA methods and breakdown at endpoint level
Step 6	Sensitivity Analysis: Influential parameters for LC3 modeling

The LCA model (step 3) follows the ISO 14040 standard [42], we conduct a cradle-to-gate analysis, corresponding to the EN 15804 A1-A3 product stage [43] (raw materials supply, transportation and manufacturing) as the structure transportation, use phase and end of life after printing depend on each application. The inputs related to the research infrastructure are excluded. The LCA is conducted in the Quebec and French contexts. Furthermore, the influence of rheological properties (viscosity, yield stress) on the shaping process contribution (energy consumption) is neglected in this study as the material impact is considerably larger than the printing process contribution [13] and data is not readily available. The effect of material properties on the pumping electricity demand could be included in a further work.

The life cycle inventory (LCI) is obtained thanks to processes directly available in Ecoinvent 3.7 Cutoff (EI), of proxy EI processes manually contextualized and of mixed processes entirely constructed (Fig. 1). More information about the LCI, including sourcing, contextualization and physical properties is specified in the next section.

The definition of the functional unit involves the printability framework (step 1), meaning test procedures for the three phases of 3D printing (pumping, deposition, buildability) along with a compressive strength criteria. These methods are described in the section 2.3. The reference flow is one cubic meter of 3D printing material with a 28-day compressive strength of 30 MPa.

2.2. Materials: hypotheses and modeling

The binder is composed of general use cement blended with 8 % silica fume (GUb-8SF) 42.5 MPa conforming to the Canadian standard CSA A3001, of calcined clay containing 80 % metakaolin (chemical formula $Al2O_3 2SiO_2$), and of limestone filler. The aggregates are kiln dried sand with a diameter inferior to 2.5 mm and the superplasticizer is polycarboxylate ether based. The composition of one cubic meter of the reference mortar resulting from a trial and error process is presented in Table 2. This material, suited for 3D printing, has a compressive strength of 30 MPa at 28 days and is not built for chlorides, sulfates or freeze-thaw exposition.

The processes and flows included in the modeling, along with their hypotheses are presented below, the life cycle inventory is depicted on the Fig. 1. An analysis of different scenarios of raw material sourcing is carried out in the section 4.

2.3. Cement type GUb-8SF

The GUb-8SF 42.5 MPa binary cement is supplied by *Ciment Quebec* and is composed of 92 % of Portland cement and 8 % of silica fume (SF), by-product of silicon and ferrosilicon alloy production. This commercially-available blend is commonly used for infrastructures in Quebec, as the use of silica fume improves the strength and durability [44]. The latter is included in the LCA model with an economic allocation based on [10]. The production unit is located in Saint-Lambert-de-Lauzon (QC, CA), at a distance of 223 km. In the French context, the product is composed of the same silica fume process and the European Portland cement market activity from EI. In any case, the mixing process of this binary blend is considered to be integrated in the conventional cement manufacturing workflow, meaning no additional mixing energy is required.

2.4. Calcined clay

The calcined clay (CC) is provided by *Whitemud Resources Inc.* and is composed of around 80 % metakaolin, the rest being crystalline quartz. It is calcined from natural kaolin clay at 750 °C in a rotary kiln into a supplementary cementitious material considered as a class N natural pozzolan in accordance with the CSA A3000 and ASTM C618 standards. The QC scenario includes a transportation distance of 2900 km from Wood mountain (SK, CA) to Montréal (QC, CA). The calcination energy

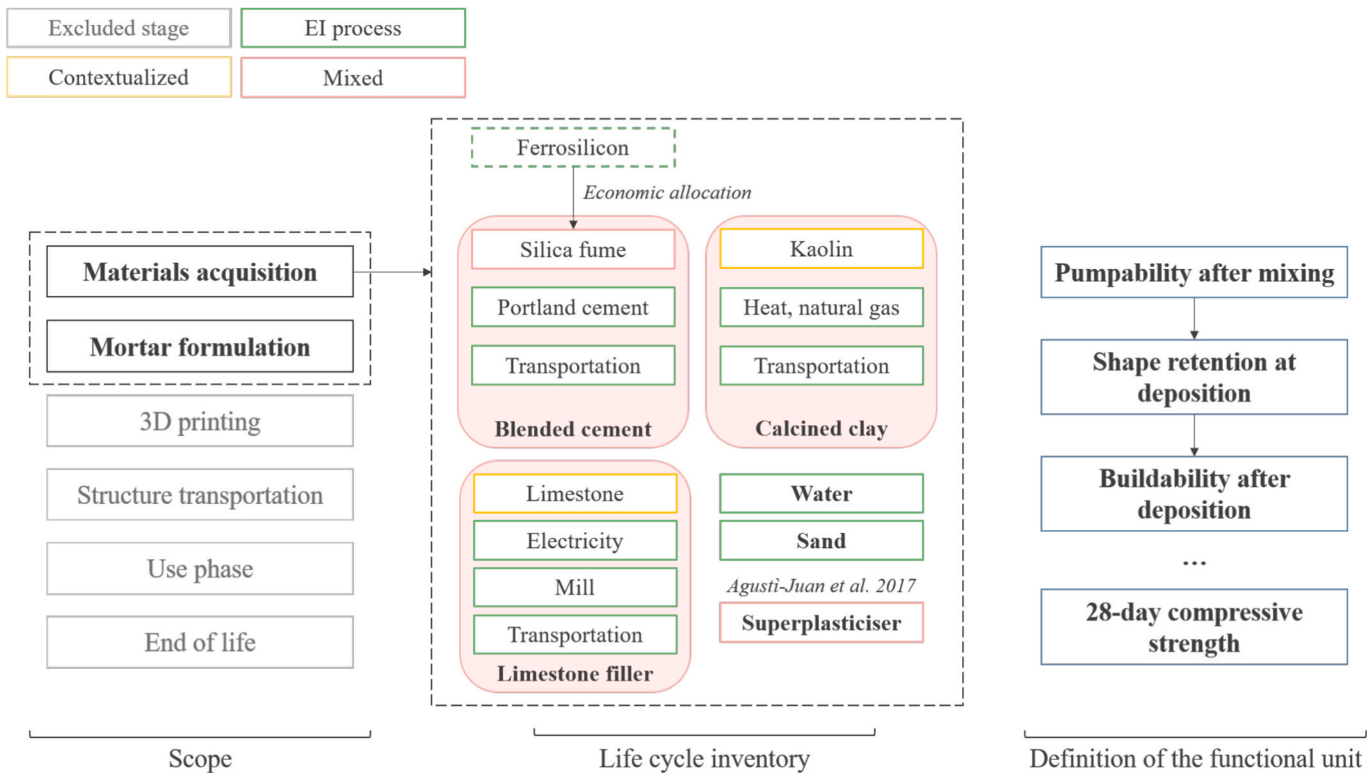

Fig. 1. Scope, life cycle inventory and requirements of the functional unit. Processes from EI, contextualization and manual integration respectively in green, yellow and pink.

Table 2
Reference mortar composition 31 MPa (LC3).

Parameter	Value
Cement GUbSF (kg)	165
Calcined clay (kg)	132
Limestone (kg)	362
Water/binder ratio	0.35
Sand/binder ratio	2
SP/binder ratio	0.01

is set at 2.6 MJ/kg [45] and subject to an analysis considering other values from the literature in the supplementary information. In the French context, a transportation distance of 535 km is selected, corresponding to a delivery from one of the main producers of CC in France which is *Imerys*, located in Clérac (17,270, France), and destined to École des Ponts ParisTech where a concrete 3D printing setup is available (535 km). For this material, a sensitivity analysis on the electricity mix, related to the location of the production plant is carried out in the QC context.

2.5. Limestone filler

The limestone filler (LF) comes from the company *Graymont* located in Portneuf (QC, CA), which constitutes a 209 km drive. The grinding data is derived from the EI quicklime production process. In the French scenario, the transportation data is derived from the transport of Portland cement in Europe, without Switzerland in EI.

2.6. Superplasticiser

The superplasticiser (SP) provided by *Master Builders Solutions* in Montreal (QC, CA) is polycarboxylate ether based and its modeling is based on [10]. In the French context, the modeling is similar.

2.7. Other materials

The other constituents are directly selected from the database EI with the Quebec version when possible, or the Rest of World (RoW) version when no Canadian version was available. Similarly, they are selected with their French version, or European if not available in the case of the French contextualization.

2.8. Modeling considerations

For the French contextualization, the amounts of exchanges in the foreground processes were identical to the Quebec setting, but the activities were contextualized to France when possible, and to Europe when no French data was found in EI. In regards to the French transportation distances of raw materials, the data from market activities were used for all foreground processes since the study is hypothetical, except for CC. For the latter, an emphasis is put since it constitutes a determining factor.

2.9. Methods

This section details the characterization tests used to assess printability and mechanical properties. It also describes the LCA tools and LCIA methods. Finally, the global analysis methodology is presented.

2.9.1. Printability, mechanical properties and life cycle assessment

2.9.1.1. Test procedures. The rheological tests are carried out at fresh state in order to cover the different stages of 3D printing. An illustration of all the test methods used as well as their function is introduced on the Fig. 2. More details on the test procedures are available in the supporting information.

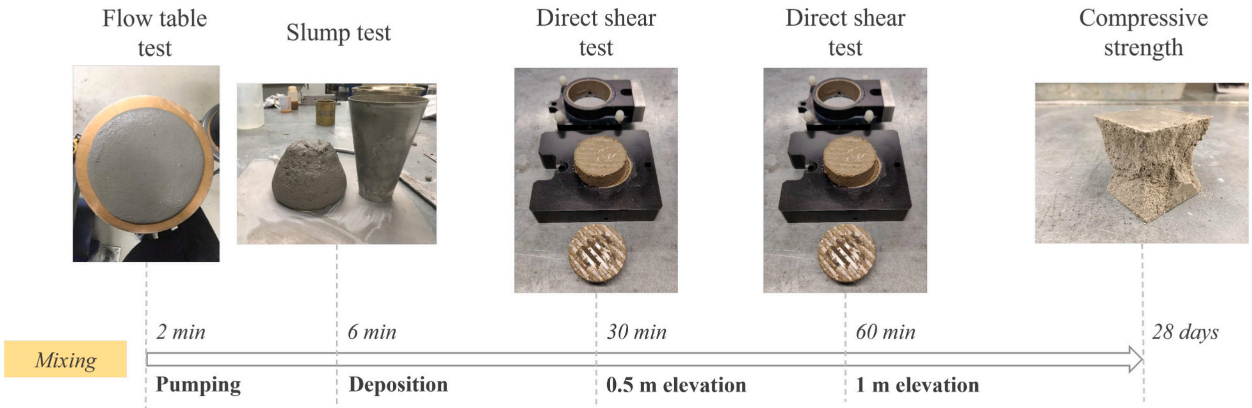

Fig. 2. Test methods and their relations to printability.

- The flow table test (standard ASTM C1437 [46]) is conducted at 2 min after mixing in order to evaluate the flowability in the pumping timeframe. A truncated cone is filled with two layers, both tampered 20 times with a rubber rod. The cone is then lifted and the table is dropped 25 times in 15 s, with a steady pace. The sum of the four measurements along the diameter lines constitutes our flow value, which is the increase in diameter as a proportion of the initial base diameter.
- The slump test (standard ASTM C143/C143M [47]) is then carried out with a miniature Abrams cone with a base diameter of 100 mm, a top diameter of 50 mm and a height of 150 mm. The mold is filled with three layers of mortar, each tampered 25 times with a steel rod. It is then lifted vertically in 5 s, letting the mortar slump under its own weight at the 6 min mark, representing the time of deposition. The yield stress for a pure elongational flow is estimated by Eq. (1) [48].

$$\tau = \frac{\rho g(H_0 - s)}{\sqrt{3}} \quad (1)$$

With τ the yield stress, ρ the density, g the gravitational constant, H_0 the initial height of the sample and s the slump.

- The rate of structuration, which is defined as the evolution of static yield stress in the dormant period (Athix for thixotropy) is measured with discrete direct shear measurements. The apparatus follows the ASTM D3080 standard [49] and the methodology is similar to [50], adapted from [51]. The mortar sample is placed in a circular shear box that restricts the horizontal strain but allows shearing on a horizontal plane where the plates of the box touch. The test is carried out at 30 and 60 min on 3 samples and the resulting static yield stress is calculated, taking into account the maximum force and the varying section of the shear box. A linear regression between these yield stress values and the slump test yield stress value gives a structuration rate in Pa/s.
- Finally, the compressive strength is determined with a hydraulic piston at a steady rate of 1 kN/S following the standard ASTM C109 [52] after a 28 day cure at 22 °C and 97.5 % relative humidity.

2.9.2. *Definition of printability thresholds*

The printability of a material is defined through multiple components and dependent on the available printing setup. In our case, the 3DPM was designed via trial-and-error for a **continuous mixing unit feeding a 1 K extrusion system**. The rheological and mechanical requirements are based either on the literature (mechanical properties, buildability) or on large-scale experiments (pumpability, shape retention), as referred to in the supporting information. These tests set the printability thresholds at 120 % flow 2 min after mixing, around 65 mm slump 4 min later, and 3.5 Pa/s structuration rate. For the mechanical properties, we consider that the mortar should remain structural. In that regard, the objective of 30 MPa constitutes a potential for high cement substitution yet structural applications, and is provided with referenced studies in the literature in terms of GWP [6,12,15].

2.9.3. *Life cycle assessment: tools and impact categories*

The LCA is conducted with the open-source software Brightway2 [53], along with its graphic interface Activity browser [54] and relies on the database Ecoinvent 3.7 Cutoff [55]. For the constitution of the characterized inventory and impact assessment, the selected methods are Environmental Footprint 3.0 recommended by the International Reference Life Cycle Data System [56]. Although the emphasis is placed on the GWP, the other midpoint indicators (Table 3) are evaluated in order to analyze the potential impact shifting from Portland cement based mortars to LC3-based mortars.

In order to quantify the influence of impact shifting at the endpoint level, we consider the endpoint LCIA methods from ReCiPe (H,A) 2016 [57] for an estimation of the damages to human health, ecosystems and resource availability. The constant midpoint to endpoint conversion factors used to calculate the scores according to Eq. (2) are listed in the supplementary information and allow an evaluation of the contribution of midpoint results to endpoint scores. The different midpoint indicators from ReCiPe 2016 over EF 3.0 are the distinction between damages to human health (PCOFhh) and ecosystems (PCOFeco) for ozone formation, the absence of terrestrial eutrophication and the presence of terrestrial ecotoxicity (TEx) and marine ecotoxicity (MEx).

$$CFe_{x,a} = CFm_x \times F_{M \to ,E,a} \quad (2)$$

Where CFe and CFm respectively stand for endpoint and midpoint characterization factors, c for the cultural perspective, a for the area of

Table 3
List of Environmental Footprint 3.0 midpoint impact categories.

Impact Category	Abbreviation	Unit
Climate change	ClCh	kg CO_2-eq
Ozone depletion potential	ODP	kg CFC-11-eq
Human toxicity, cancer effects	CE	CTUh
Human toxicity, non-cancer effects	nCE	CTUh
Particulate matter/Respiratory inorganics	RE	Disease Incidences
Ionizing radiation, human health	IR	kBq U-235
Photochemical ozone formation	PCOF	kg NMVOC eq
Acidification	Ac	mol H^+-eq
Eutrophication, terrestrial	TEu	mol N-eq
Eutrophication, aquatic freshwater	FEu	kg P-eq
Eutrophication, aquatic marine	MEu	kg N-eq
Ecotoxicity freshwater	FEx	CTUe
Land use	LU	Soil Quality Index
Water use	WU	kg world eq. deprived
Resource use, minerals and metals	RMM	kg Sb-eq
Resource use, energy carriers	RF	MJ

protection, x for the stressor of concern and $F_{M\rightarrow,E,a}$ for the conversion factor.

2.10. Sensitivity analysis

In the sensitivity analysis, the focus is put on the transportation of the binder components as well as the electricity mix for clay production as these parameters represent sensitive inputs according to production location. Since the production of cement and limestone filler is extensively developed throughout Canada, the US and France, the focus is put on the locations of CC production. In the case of kaolin clay, although the resources are abundant throughout the world, and sufficient to meet global cement demand [24], the process of calcination is relatively uncommon in Canada. Several production locations are investigated and the GWP results are represented with appropriate transportation and electricity mix in order to give an estimation of calcined clay impact variability around QC. To this purpose, several commercially available calcined kaolin clays were collected, along with their freight distance and the electricity mix of their regions (Table 4). With this information, the variability of LC3 modeling, mainly affected by the variability of calcined clay modeling, is discussed.

3. Results

The objective of this study is to evaluate the GWP of an LC3 composite with high cement replacement in order to assess its potential for industry-wide use. The LC3 mixture (Table 2) constitutes the material analyzed in the following parts. This product was modeled with a set of generic processes, then contextualized in CA-QC and FR contexts according to the location-dependent variables detailed in the section 2.2.

Throughout the study, the introduced models are compared to an OPC-based (without SCM) concrete reported in the literature [12]. The latter was selected from a literature review (see supporting information) as demonstrating printability and a 30 MPa compressive strength. It was then modeled in the Quebec and France contexts to provide reference points in terms of environmental impacts.

The results breakdown is depicted on the Fig. 3. First, the GWP results are detailed, including a contribution analysis. The contextualizations in Quebec and France illustrate the environmental impacts variability in 3D printing LC3 application. The results from other midpoint indicators are detailed for both contexts and the processes responsible for the impact shifting are specified.

3.1. Global warming potential and contribution analysis

The process contributions of the OPC 3DPM as well as our LC3 mixture contextualized in Quebec and France (respectively OPC QC, OPC FR, LC3 QC and LC3 FR) are represented on the Fig. 4. OPC-based models display comparable CO_2 emissions. For a similar compressive strength of 30 MPa at 28 days, LC3 demonstrates a decrease of 36 % in GWP in the QC context and 46 % in the FR context. As expected, the majority of the estimated LC3 GWP stems from the OPC in the mixture (53.6 %) although accounting for only 6.8 wt% of the mixture. Concerning the impact of the calcined clay, which is the specificity of LC3, the Fig. 4 shows a contribution of 34 % to the total LC3 QC ClCh score. When considering LC3 FR, while the GWP of GUbSF remains similar, the main differences reside in the ClCh scores of CC and LF. An 81.2 % drop is observed for the LF foreground process, mainly due to the reduced impact related to the transportation. Concerning the CC, both the production of kaolin and the production of natural gas generate far more GHG emissions in the Canadian context, or more precisely the SK setting (respectively 2.4 and 2.3 times the GWP of the French version). On the contrary, the GWP related to the transportation of CC is halved in Canada since it is modeled with a train as opposed to a lorry in the French context. In the end, the 130 kg of CC induce respectively 86 and 69 kg CO_2-eq in the Quebec and the French context according to the models *LC3 QC* and *LC3 FR* used in this study.

It is observed that as the cement substitution increases, which is the final objective of this study, the GWP associated to CC is more decisive. When considering only the production without the transportation in the QC scenario, the impact factor of GUbSF and CC are respectively 0.79 kg CO_2-eq and 0.51 kg CO_2-eq. The production of kaolin with an electricity mix from SK, CA, and the natural gas needed to dehydroxylate the kaolin account for respectively 45 % and 32 % of the total CC impact. The significant impact of CC in our model, although lower than OPC, is also amplified by the distance of 2900 km considered in this study which represents 23 % of the CC impact whereas the transportation-related GWP in the GUbSF is only 3.7 % of its total impact.

Table 4
List of commercially available kaolin clays in the vicinity of Quebec, Canada and a French case.

Location	Electricity mix [58,60]	Freight modes: distances (km) [59]	Comments
Wood Mountains, SK, CA	Coal and coke: 41 % Natural gas: 40 % Hydro: 15 % Other renewable: 4 %	Lorry: 68 Train: 2800	2017 SK electricity mix Freight to ETS Montreal
Sandersville, GA, USA	Coal and coke: 32 % Natural gas: 34 % Nuclear: 12 % Hydro: 8 % Other non-renewable: 10 % Other renewable: 4 %	Lorry: 207 Cargo: 2088	2014 SERC region electricity mix Sea freight distance based on, Distances *National Oceanic and Atmospheric Administration* 2019 Freight to ETS Montreal
Aiken County, SC, USA	Coal and coke: 32 % Natural gas: 34 % Nuclear: 12 % Hydro: 8 % Other non-renewable: 10 % Other renewable: 4 %	Lorry: 203 Cargo: 2014	2014 SERC region electricity mix Sea freight distance based on *National Oceanic and Atmospheric Administration, Distances* 2019 Freight to ETS Montreal
High Hill, MO, USA	Coal and coke: 32 % Natural gas: 34 % Nuclear: 12 % Hydro: 8 % Other non-renewable: 10 % Other renewable: 4 %	Lorry: 20 Train: 1660	2014 SERC region electricity mix Freight to ETS Montreal
Clerac, 17,270, France	Coal and coke: 3 % Natural gas: 7 % Nuclear: 72 % Hydro: 10 % Other renewable: 9 %	Lorry: 535	2017 FR electricity mix Freight to École des Ponts Paris Tech

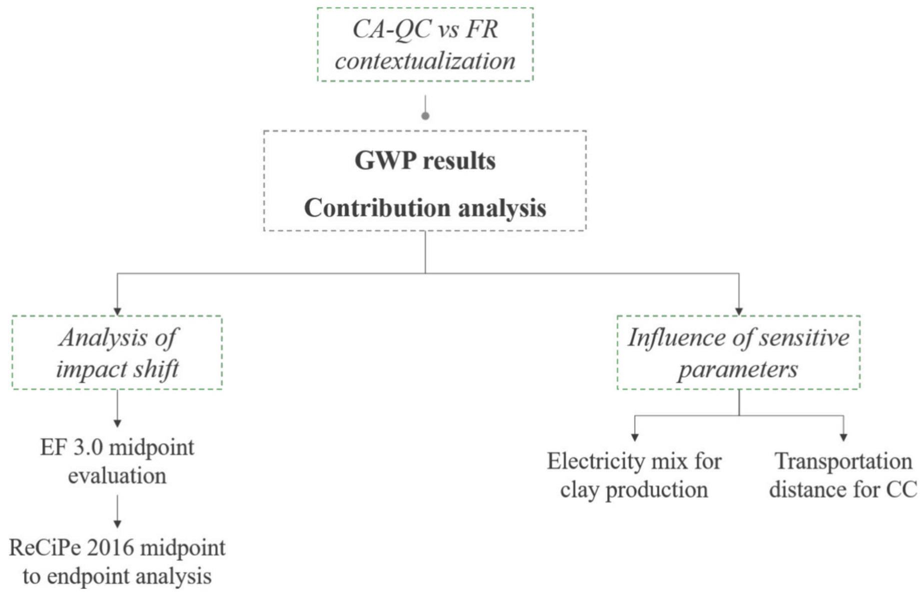

Fig. 3. Result analysis methodology.

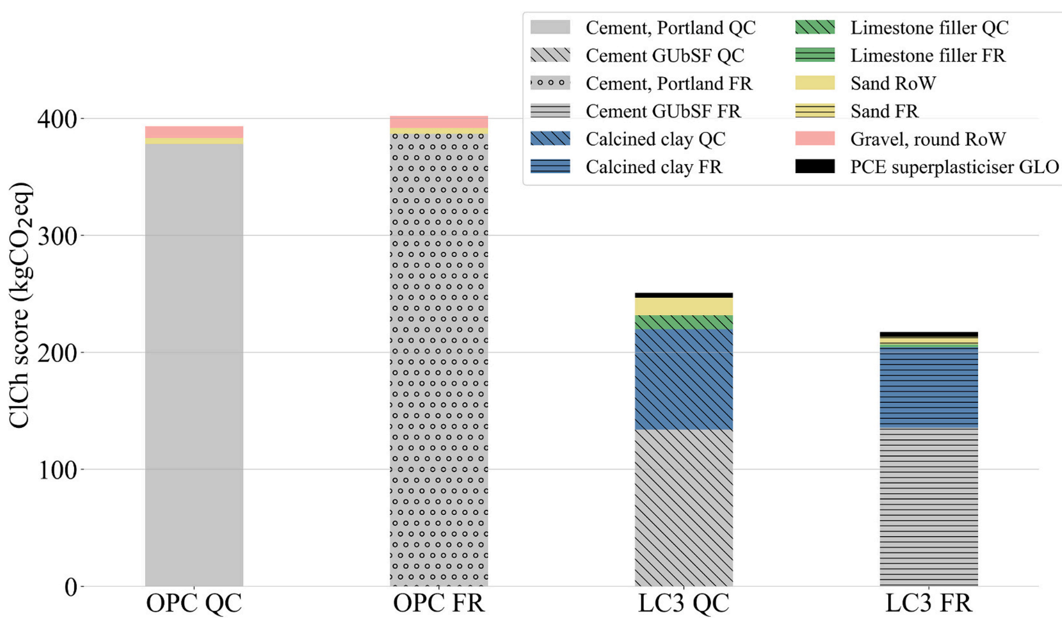

Fig. 4. Process contribution of all models from left to right: Literature model [12] reproduced in the Quebec (OPC QC) and French (OPC FR) contexts; LC3 model contextualized in Quebec (LC3 QC) and France (LC3 FR).

3.2. Assessment of impact shifting

This section provides results over a comprehensive set of impact categories for the three models in order to evaluate the validity of a GWP focus in case of a subsequent material optimization. The scores for each midpoint indicator listed in the Table 1 are represented on the Fig. 5 for models OPC QC (grey), OPC FR (blue), LC3 QC (green) and LC3 FR (red). In total, the LC3 QC scenario shows an increase of score in 6 out of 16 indicators compared to the OPC QC from the literature, namely ozone depletion potential, carcinogenic effects, ionizing radiation, freshwater eutrophication, land use and energy carrier use. The other categories display a similar or decreased score with a substantial reduction for climate change, photochemical ozone formation, acidification, terrestrial eutrophication, marine eutrophication, freshwater ecotoxicity as well as minerals and metals use.

In the French case, the LC3 displays an increase in 5 out of 16 indicators compared to OPC. Three of these are identical to the QC case (ODP, IR, RF) and two are different (RE, FEu). When comparing LC3 in both contexts, the LC3 FR model presents a reduced impact in 13 out of 16 indicators compared to LC3 QC. Moreover, out of these 13 indicators, 11 show a substantially decreased score (> 10 %).

For each indicator affected negatively in either contexts, the predominant processes resulting in a superior score for LC3 compared to OPC can be identified:

- **ODP**: the contribution of the long distance transport of natural gas via pipeline is the main contributor (34 %), followed by the production of natural gas, high pressure, explain the higher score of LC3 in QC;

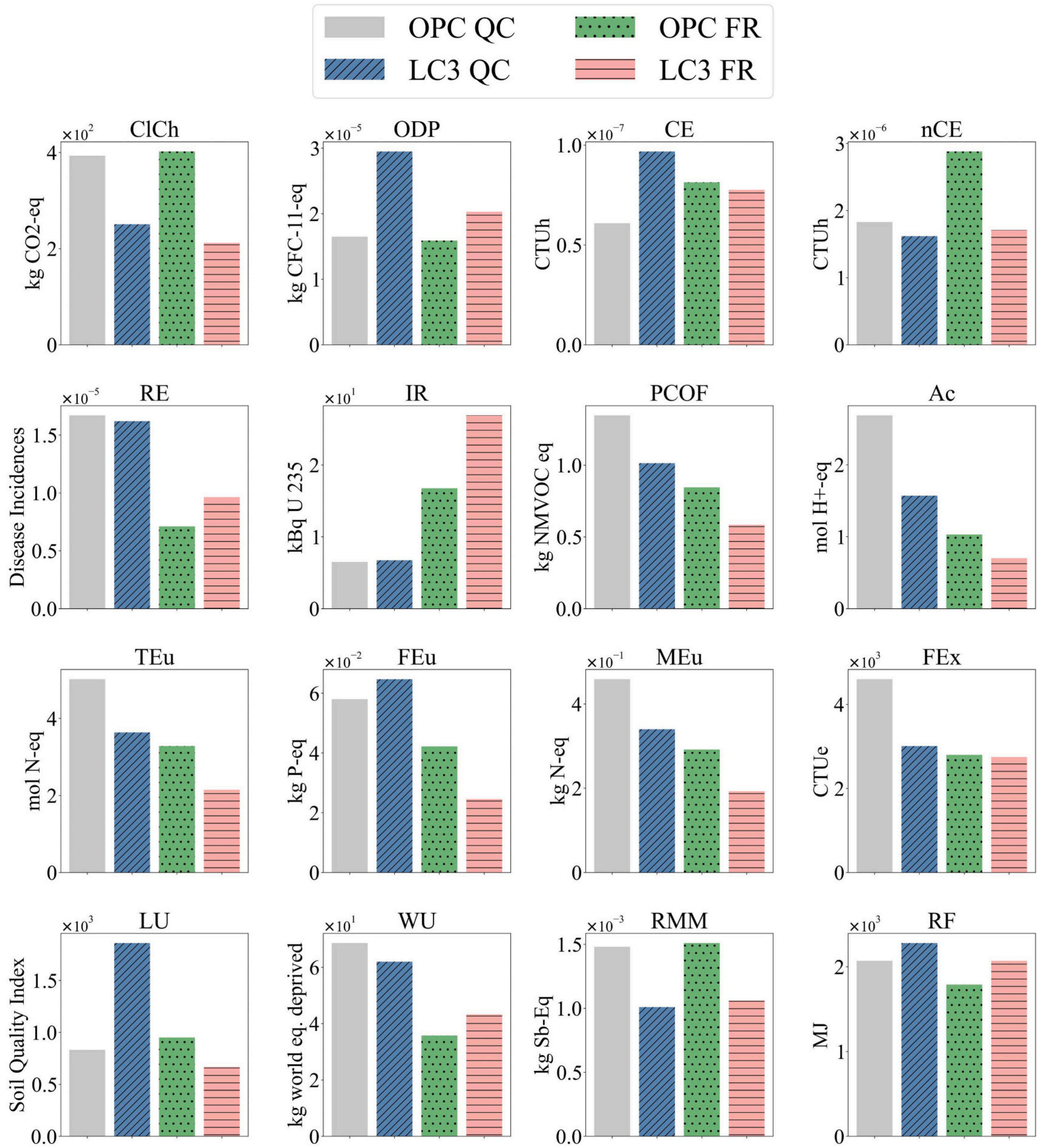

Fig. 5. Results of Environmental Footprint 3.0 impact categories (Table 1) for models of printable OPC and LC3 based mixtures in QC and FR contexts.

- **CE**: the treatment of electric arc furnace slag and the production of coke involved in the construction of railway tracks in low-alloyed steel (CC transportation) contribute to the higher score of the model LC3 QC;
- **RE**: the contribution of the silica fume production explains the increase in disease incidences for LC3 over OPC in the FR context;
- **IR**: the contribution of the tailing from uranium milling is responsible for the slightly higher score of LC3 QC over OPC QC. When comparing LC3 in FR over QC, the 300 % increase is due to the largely predominant nuclear energy in the French electricity mix;
- **FEu**: the contribution of the spoil from lignite mining (56 %) is largely responsible for the slight increase in FEu score in QC;
- **LU**: contrary to the OPC QC mixture which contains gravel and sand, the LC3 mixture contains only sand in higher quantity. The sand quarry operation, extraction from river bed explains the increase in LU score for our LC3 mixture;
- **WU**: the kaolin production process accounts for 16 % of the WU score for LC3 FR and is therefore responsible for the greater impact over the OPC based model;
- **RF**: a collection of processes pertaining to the CC contributes to the higher score of LC3, however, the main contribution remains the natural gas production, high pressure (17.6 % of the total score in the QC context).

When displaying the process contributions for the model LC3 QC across all impact categories on the Fig. 6, we can observe that apart from the LU indicator for which a majority of the score is attributed to the sand, the other impact categories are mainly affected by the GUbSF and the CC. The significant influence of the CC represented in blue explains the impact shift for certain categories.

3.3. Endpoint assessment

The study of potential impact shifting reveals the key role played by the amount of natural gas involved in the calcination of clay, especially for the indicators ODP and RF. A complementary review of the different values of energy demand in the literature is available in the supporting information [45,61,62]. In order to determine if the superior score

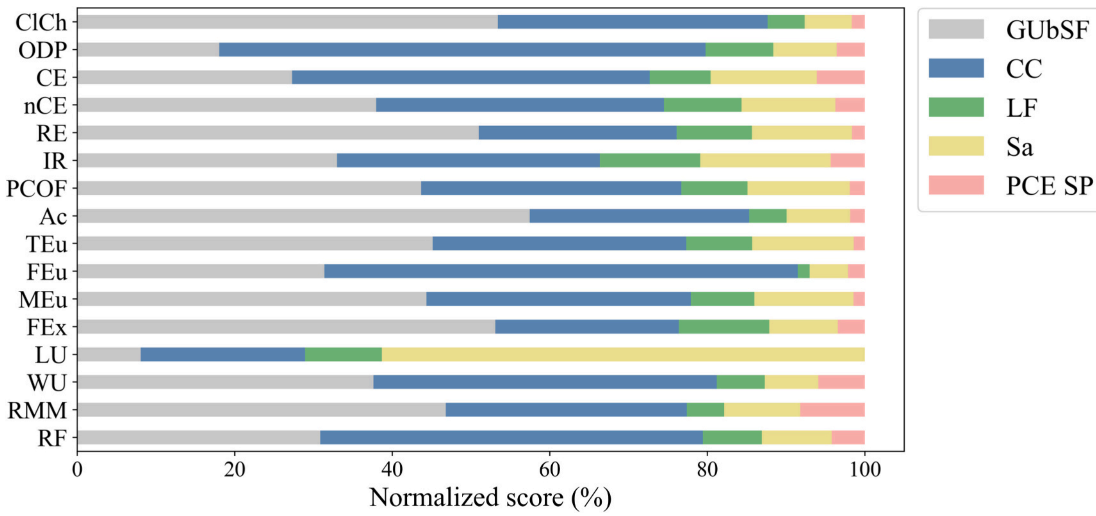

Fig. 6. Process contributions for all impact categories in Table 1 for the LC3 QC model.

observed in 6 out of 16 categories constitutes a barrier in the use of 3DP LC3, these results are analyzed at the endpoint level. The aggregated endpoint results for human health, ecosystems and resources are detailed in the Table 5.

This table shows the decrease of impacts on human health (QC: -31 %; FR: −39 %) and ecosystems (QC: -30 %; FR: −43 %) for LC3 over OPC based 3DPM. On the contrary, the impact on resources is higher (QC: +54 %; FR: +24 %). When taking the single score assessment of ReCiPe 2016, LC3 still improves the environmental scores in both QC and FR contexts (QC: -22 %; FR: −33 %), which highlights the prevailing of LC3 environmental improvements over the impact shift attributed to the production of calcined clay. In order to substantiate this statement, a breakdown of the contributions of midpoint impact categories to aggregated endpoint indicators is represented for human health, ecosystems and resources respectively on Figs. 7, 8 and 9, displaying the following trends:

- **Human health**: 49 % of the impact is attributed to the ClCh in QC (60–70 % in FR), which experiences a reduction of 36 % (46 % in FR) for LC3 compared to OPC. The majority of the remaining impact is attributed to the particulate matter formation (RE) category, for which there is also a decrease for LC3. Thus, the increases observed for LC3 constitute less than 0.7 % of the damage to human health.
- **Ecosystems**: the terrestrial and freshwater impacts are lower for LC3 whereas the marine influence is greater. However, the Fig. 8 shows a minor contribution of marine indicators to total ecosystems footprint, which explains the decreased overall ecosystems score of LC3 over OPC in both geographical contexts.
- **Resource availability**: the LC3 score is higher than OPC in both contexts. When considering a higher level of aggregation, the impact increase for LC3-based 3DPM is overall balanced by the decrease in other impact categories, especially in the range of human health.

Table 5
ReCiPe 2016 aggregated endpoint assessment for all models.

Model	Human health (DALY)	Ecosystems (species. yr)	Resources (USD 2013)
OPC QC	7.4×10^{-4}	1.7×10^{-6}	1.3×10^{1}
LC3 QC	5.1×10^{-4}	1.2×10^{-6}	1.9×10^{1}
OPC FR	5.3×10^{-4}	1.4×10^{-6}	1.2×10^{1}
LC3 FR	3.3×10^{-4}	8.2×10^{-7}	1.5×10^{1}

4. Discussions

4.1. Comparison with LC3 studies

Four studies containing mixture proportions for printable LC3 materials are assessed using our CA-QC LCA model in the Table 6. The 251 kg CO_2-eq/m^3 mark for a 31 MPa concrete studied in this paper stands well below the existing 3D printable 1 K materials in the literature, even when considering kg CO_2-eq/m^3/MPa. Naturally, durability must be considered to assess the whole life cycle and location-dependent parameters will significantly influence the results. A way to enhance the resistance of our material would be to partially calcine the limestone, providing additional portlandite to support the pozzolanic reaction of calcined clay [63,64] in a low-clinker system.

4.2. LC3 sensitive parameters

The results of process contribution for CC highlight the need for a minimization of cement content, but also an optimization of CC content for a desired shaping process and compressive strength. The trial and error process carried out in order to define a functional unit reflected this result as the GUbSF and CC content were adjusted from the existing literature which recommends a binder composition of 50 % cement, 30 % calcined clay, 15 % limestone and 5 % gypsum [24,25]. However, further studies concerning the durability of such mixtures are necessary in order to account for the whole life cycle.

The parameters presenting a significant variability according to the study location are the transportation modes and distances as well as the electricity mix for CC production. The GWP differences between the scenarios in Table 4 are represented on the Fig. 10 for the supply of 1 ton of CC. This figure highlights the significant impact of CC sourcing as a decrease of 42 % in ClCh score is observed in the case of Georgia (US) or South Carolina (US) based suppliers. For these two locations, the GWP linked to transportation and medium voltage electricity for kaolin production decrease by respectively 68 % and 22 %. Overall, the actual case of this study (CA-SK) generates the most GHG emissions. A drop in the GWP of medium voltage electricity is observed in the French case, owing to the minor amount of lignite-based high voltage electricity production in France. Conversely, the GWP related to transportation is much higher than the other locations since it is modeled with a lorry on the entire distance.

These differences in CC CO_2 emissions translate into a variability of up to 15 % in the total score of LC3 mixtures. Considering the CC accounts for less than 6 % of the total mortar mass, these parameters are

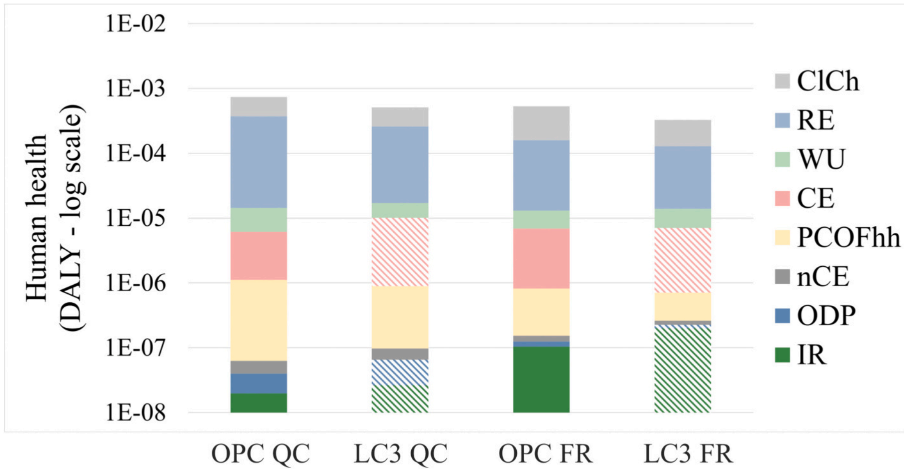

Fig. 7. Midpoint contributions to aggregated human health for models OPC QC, LC3 QC, OPC FR and LC3 FR: striped sections represent categories for which LC3 > (OPC)

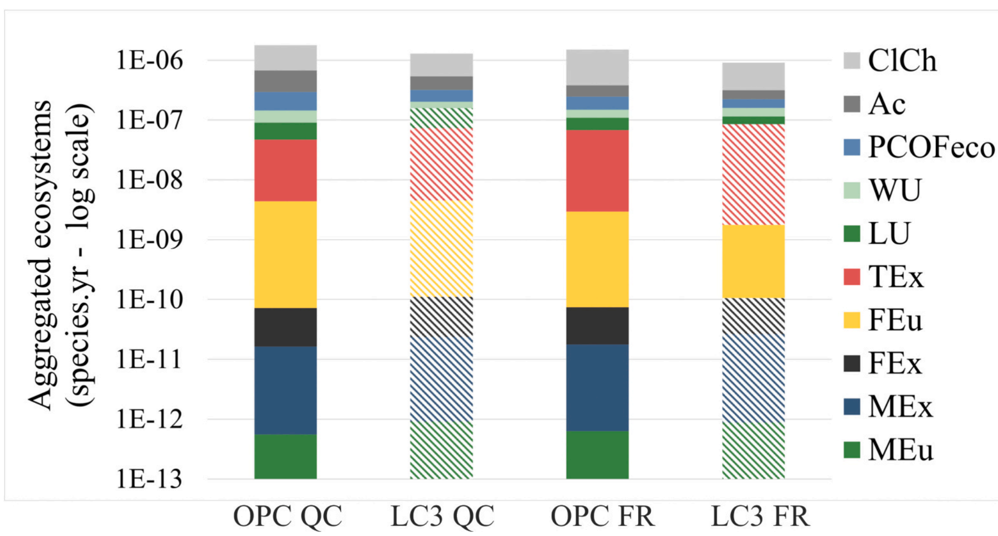

Fig. 8. Midpoint contributions to aggregated ecosystems for models OPC QC, LC3 QC, OPC FR and LC3 FR: striped sections represent categories for which LC3 > (OPC)

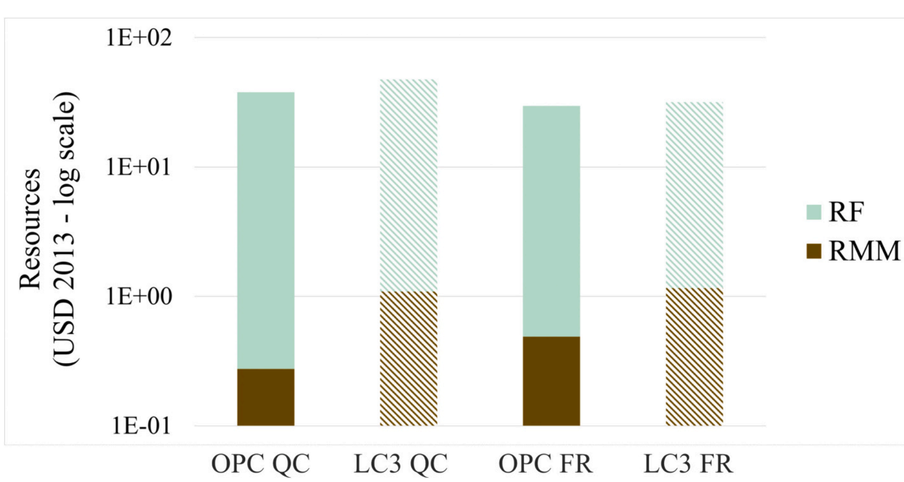

Fig. 9. Midpoint contributions to aggregated resources for models OPC QC, LC3 QC, OPC FR and LC3 FR: striped sections represent categories for which LC3 > (OPC)

Table 6
Comparison with other 3D printable LC3 reported in the literature: Calculated GWP exclude admixtures other than superplasticizers.

Authors	Composition	Compressive strength 28 days (MPa)	Reported GWP (kg CO_2-eq/ m^3)	Calculated GWP in CA-QC context (kg CO_2-eq/ m^3)
Ibrahim et al. [35]	LC3	30		534
Bhattacherjee et al. [62]	LC3	35	314	364
Long et al. [32]	LC3 + SF	37	283	366
Chen et al. [33]	LC3	40		554

indeed determining factors for the total GWP. Thus, a emphasis on the use of local materials can allow a significant saving in GWP. This indicates that in the case of a sharp increase in LC3 use, the locations of the CC production plants should be determined in order to minimize the averaged transportation distances while avoiding as much as possible the territories relying mainly on fossil fuels for electricity production. In the future, and depending on the availability of kaolin resources, a parameterized analysis on the transportation distance and the location of the production plant could allow a reduction of total impacts for each location of LC3 use.

As a way to enhance the validity of this study, an additional French source of LCA data is considered. The project DIOGEN, initiated by the *Association Française de Génie Civil* gathers academic and industrial actors with the objective of establishing a database identifying the environmental impacts of the materials used in the construction industry. Originating directly from industrial partners operating real processes, values of environmental impacts are estimated according to the French norm NF EN 15804/CN. If we consider only the production of CC, the model included in DIOGEN, which involves the production of metakaolin calcined in a rotary kiln by *Imerys*, the total ClCh score is evaluated at 239 kg CO_2-eq/ton whereas the present study estimates the CC GWP to be respectively 508 kg CO_2-eq/ton and 210 kg CO_2-eq/ton in the Quebec and French contexts. In France, the model of CC in our study and the dataset originating directly from a CC producer generate similar results which validates the hypotheses related to the production and calcination of kaolin clay in this study. As the process is designed identically in Quebec and considering similar values from the literature mean values found in the literature [45,66,67], the consistency of this model is confirmed.

4.3. Industrial implementation, upscale scenario and kaolin clay availability

In terms of practical implications for LC3 in the concrete 3D printing industry, limestone and clay are globally available and LC3 is cost-effective [68]. However, the mix design is more complex and the use of OPC is so widely spread that economical incentives are essential for the adoption of high SCM concretes. Nevertheless, as the 3D printing industry is in development, this type of material is well-suited, as volumes are reduced and tailor-made materials are very common.

In the case of a sharp increase in LC3 use, the availability of materials (kaolin clay) and energy (electricity for kaolin clay extraction, natural gas for calcination) allocated to calcined clay production, which constitutes the most critical component, needs to be assessed. The present study could be complemented by the modeling of the conjectural additional demand in energy and materials according to exchanges in the adequate markets (North American, European). Finally, the rebound effect needs to be reflected upon as the additional LC3 3DPM produced may add to the existing 3DP OPC-based material use instead of replacing it.

The distribution of clay-size minerals on land for topsoil and subsoil is represented in [69]. It indicates an abundance of kaolin clay in the Chinese, African and South American regions as well as considerable amounts in the United States of America (east and central) and East Europe. In Canada, the interior system Cordilleran, the Artic and the Appalachian regions have reported kaolinitic deposits [70]. However, the reported mining operations are generally located in SK. In the vicinity of Quebec, the most active kaolinitic clay production is located in Georgia (USA) but kaolin deposits have been reported in the states of Pennsylvania (USA) around the Piedmont physiographic province, of West Virginia (USA) associated with the Appalachian region, or in Virginia (USA).

The use of lower grade kaolinitic clay is adequate for the production of LC3 [71], making the suitable clay reserve larger, although the higher grade kaolinitic clays provide enhanced structuration rate highlighting a need for the determination of an minimal grade in the context of 1 K 3D printing.

4.4. Data quality

In this study, the technologies considered in the production of the

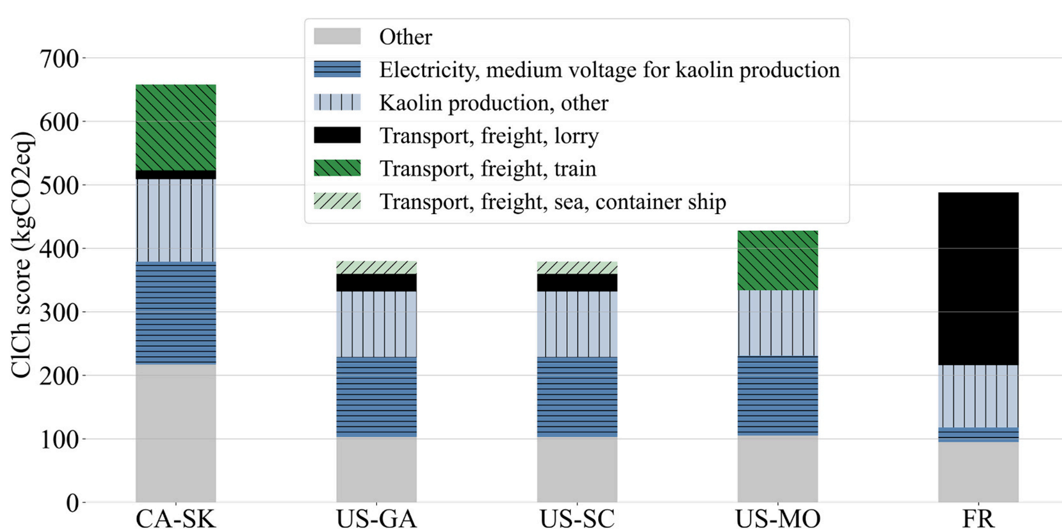

Fig. 10. Process contribution for the supply of 1 ton of CC from the production locations in Table 4.

different raw materials are the only ones available in EI. The modeling of the production of OPC in QC is based on data corresponding to 2007 inventory, output and capacity utilization rate. Furthermore, the production of kaolin is also modeled with 2007 data from one single company in Europe and its calcination method is the rotary kiln. Considering these information, uncertainties regarding the relevance of the data could arise. Indeed, processes have evolved since 2007 and more efficient technologies of production have been implemented. Particularly, *Ciment Quebec* integrates an extended preheater and a short rotary kiln that generate fewer GHG compared to the Quebec average cement production. Also, according to the database DIOGEN and the CC producer *Imerys*, the flash calcination of kaolin clay allows a significant reduction of energy consumption, which results in a ClCh score of 139 kgCO_2-eq/ton compared to the 239 kg CO_2-eq/ton estimated for rotary kiln metakaolin. Naturally, the calcination process also affects other properties of the material such as reactivity or water absorption. In the same way, the heat used for clay calcination is modeled with shares of production methods for industrial sectors in Quebec (or Europe in the French context), but if we consider that the heat comes from a co-generation in a conventional power plant in SK, the ClCh contribution of the industrial heat from natural gas could be three times lower. We can imagine even more favorable scenarios with the use of biogas from agricultural waste for instance. These examples show the substantial influence of the technological state and could be the subject of a deeper analysis considering the best and worst cases to date.

4.5. Cradle-to-gate limitations

In order to be able to assess the comprehensive environmental impacts of the low-clinker 3DPM developed in this study, the printing process, distribution phase, use phase, and end of life need to be considered. Specifically, durability tests such as resistance to chloride penetration, sulfate attack or freeze-thaw have to be performed and compared to OPC-based 3DPM. Besides, the modularity potential of 3D printing also needs to be considered at the end of life stage for reuse or repurposing. Overall, the application to several use cases such as structurally optimized beams, façades or lost formwork [72] over their entire life cycle is required in order to consider a holistic approach for comparison between conventional and digital concrete, but also between OPC and LC3 materials.

Following this study, the objective is to integrate an LCA calculation in the multi-objective optimization of a sustainable 3DP mortar. In that regard, a consideration of mechanical and durability performance will be included in the optimization, thus allowing us to propose a complete tool for designing low-impact 3DP mortars.

5. Conclusion

In order to evaluate the relevance of LC3 for low-carbon 3D printing, the 3D printable LC3-based material developed in this study has been compared to a reference Portland cement-based 3D printing mortar with the same compressive strength. Two novel use-cases (Montreal, CA-QC; Champs-sur-Marne, FR) have been explored and a sensitivity analysis on calcined clay suppliers has been carried out.

- A climate change score reduction of respectively 36 % and 46 % are observed for the Quebec and French model.
- Score increases are experienced in 6 out of 16 indicators (ODP, CE, IR, FEu, LU and RF), mainly attributed to the natural gas for clay calcination as well as calcined clay transportation over long distances. However, when considering the damages to human health, ecosystems and resource availability, the decrease in most indicators prevails over the increase in the aforementioned impact categories. In the French context, the reduction in environmental impacts for LC3 is more apparent with substantial improvements in 11 out of 16 impact categories compared to the Quebec scenario.
- An additional 15 % of ClCh score decrease could be expected solely from the sourcing of more local calcined clay. As the calcined clay industry is less developed than the globally uniform cement industry, the availability of kaolinitic clay, meaning the transportation distance is to be evaluated before assuming a replacement is environmentally worth it, although the macroscopic properties related to 3D printing can justify it.
- In addition to that, the electricity mix plays a more predominant role in the production of clay compared to cement, making the global warming potential reduction all the more dependent on LC3 use location.

In the context of 3D printing, the use of LC3 is a viable solution for the reduction of environmental impacts compared to OPC-based materials when the mix design is adequate. However, a quantification of mechanical and durability properties are required in order to consider the whole life cycle of a 3D printed structure, including use phase and end of life. For the material acquisition phase, a future study modeling the conjectural additional demand in energy and materials for the generalization of calcined clay use considering the distribution of clay minerals and specific energy mixes could accelerate the adoption of LC3.

With the parametric LCA model constructed in this study, the minimization of the climate change score will be used as an objective function for the optimization of low-carbon 3D printing materials. This further study will propose an automated, reproducible tool for the tuning of material properties from fresh to hardened using local raw materials.

CRediT authorship contribution statement

Willy Jin: Writing – original draft, Software, Methodology, Data curation, Conceptualization. **Charlotte Roux:** Writing – review & editing, Methodology, Conceptualization. **Claudiane Ouellet-Plamondon:** Writing – review & editing, Supervision, Resources, Methodology, Funding acquisition, Conceptualization. **Jean-François Caron:** Writing – review & editing, Supervision, Funding acquisition, Conceptualization.

Declaration of competing interest

The authors declare that they have no known competing financial interests or personal relationships that could have appeared to influence the work reported in this paper.

Data availability

Data will be made available on request.

Acknowledgements

The authors would like to thank the Canada research chairs program (CRC-2019-00074), the Natural Sciences and Engineering Research Council of Canada and the LABEX MMCD (ANR-11-LABX-0022) for funding this research.

Appendix A. Supplementary data

Supplementary data to this article can be found online at https://doi.org/10.1016/j.susmat.2024.e01119.

References

[1] J. Xiao, G. Ji, Y. Zhang, G. Ma, V. Mechtcherine, J. Pan, L. Wang, T. Ding, Z. Duan, S. Du, Large-scale 3D printing concrete technology: current status and future opportunities, Cem. Concr. Compos. 122 (Sept. 2021) 104115.

[2] B. García de Soto, I. Agustí-Juan, J. Hunhevicz, S. Joss, K. Graser, G. Habert, B. T. Adey, Productivity of digital fabrication in construction: cost and time analysis of a robotically built wall, Autom. Constr. 92 (Aug. 2018) 297–311.
[3] M.S. Khan, F. Sanchez, H. Zhou, 3-D printing of concrete: beyond horizons, Cem. Concr. Res. 133 (July 2020) 106070.
[4] R.J. Flatt, T. Wangler, On sustainability and digital fabrication with concrete, Cem. Concr. Res. 158 (Aug. 2022) 106837.
[5] I. Muñoz, J. Alonso-Madrid, M. Menéndez-Muñiz, M. Uhart, J. Canou, C. Martin, M. Fabritius, L. Calvo, L. Poudelet, R. Cardona, H. Lombois-Burger, N. Vlasopoulos, C. Bouyssou, J. Dirrenberger, A. Papacharalampopoulos, P. Stavropoulos, Life cycle assessment of integrated additive–subtractive concrete 3D printing, Int. J. Adv. Manuf. Technol. 112 (Feb. 2021) 2149–2159.
[6] I. Agustí-Juan, G. Habert, Environmental design guidelines for digital fabrication, J. Clean. Prod. 142 (Jan. 2017) 2780–2791.
[7] R.M. Andrew, CO_2, Earth Syst. Sci. Data 10 (Jan. 2018) 195–217. Publisher: Copernicus GmbH.
[8] K. Richardson, W. Steffen, W. Lucht, J. Bendtsen, S.E. Cornell, J.F. Donges, M. Drüke, I. Fetzer, G. Bala, W. von Bloh, G. Feulner, S. Fiedler, D. Gerten, T. Gleeson, M. Hofmann, W. Huiskamp, M. Kummu, C. Mohan, D. Nogués-Bravo, S. Petri, M. Porkka, S. Rahmstorf, S. Schaphoff, K. Thonicke, A. Tobian, V. Virkki, L. Wang-Erlandsson, L. Weber, J. Rockström, Earth beyond six of nine planetary boundaries, Sci. Adv. 9 (Sept. 2023) eadh2458. Publisher: American Association for the Advancement of Science.
[9] C. Roux, K. Kuzmenko, N. Roussel, R. Mesnil, A. Feraille, Life cycle assessment of a concrete 3D printing process, Int. J. Life Cycle Assess. 28 (Nov. 2022) 1–15.
[10] I. Agustí-Juan, F. Müller, N. Hack, T. Wangler, G. Habert, Potential benefits of digital fabrication for complex structures: environmental assessment of a robotically fabricated concrete wall, J. Clean. Prod. 154 (June 2017) 330–340.
[11] S. Maitenaz, R. Mesnil, P. Onfroy, N. Metge, J.-F. Caron, Sustainable Reinforced Concrete Beams: Mechanical Optimisation and 3D-Printed Formwork, in: Second RILEM International Conference on Concrete and Digital Fabrication, RILEM Bookseries, Springer, Cham, July 2020.
[12] Y. Han, Z. Yang, T. Ding, J. Xiao, Environmental and economic assessment on 3D printed buildings with recycled concrete, J. Clean. Prod. 278 (Jan. 2021) 123884.
[13] K. Kuzmenko, N. Gaudillière-Jami, A. Feraille, J. Dirrenberger, O. Baverel, Assessing the environmental viability of 3D concrete printing technology, in: Design Modelling Symposium Berlin, Springer, Cham, Jan. 2020, pp. 517–528.
[14] M.W. Tait, W.M. Cheung, A comparative cradle-to-gate life cycle assessment of three concrete mix designs, Int. J. Life Cycle Assess. 21 (June 2016) 847–860.
[15] A. Béton Québec, Association béton Québec (ABQ) Industry-Wide EPD for Ready-Mixed Concrete, July 2022.
[16] N. Roussel, Rheological requirements for printable concretes, Cem. Concr. Res. 112 (Oct. 2018) 76–85.
[17] C. Zhang, Z. Hou, C. Chen, Y. Zhang, V. Mechtcherine, Z. Sun, Design of 3D printable concrete based on the relationship between flowability of cement paste and optimum aggregate content, Cem. Concr. Compos. 104 (Nov. 2019) 103406.
[18] N. Roussel, A thixotropy model for fresh fluid concretes: theory, validation and applications, Cem. Concr. Res. 36 (Oct. 2006) 1797–1806.
[19] Y. Chen, F. Veer, O. Çopuro, A critical review of 3D concrete printing as a low CO2 concrete approach, Heron 62 (2017) 167–194.
[20] H. Alhumayani, M. Gomaa, V. Soebarto, W. Jabi, Environmental assessment of large-scale 3D printing in construction: a comparative study between cob and concrete, J. Clean. Prod. 270 (Oct. 2020) 122463.
[21] M.P. Tinoco, E.M. de Mendonça, L.I.C. Fernandez, L.R. Caldas, O.A.M. Reales, R. D. Toledo Filho, Life cycle assessment (LCA) and environmental sustainability of cementitious materials for 3D concrete printing: A systematic literature review, J. Build. Eng. 52 (July 2022) 104456.
[22] C. Orozco, S. Babel, S. Tangtermsirikul, T. Sugiyama, Comparison of environmental impacts of fly ash and slag as cement replacement materials for mass concrete and the impact of transportation, Sustain. Mater. Technol. 39 (Apr. 2024) e00796.
[23] V.K. Singh, G. Srivastava, Development of a sustainable geopolymer using blast furnace slag and lithium hydroxide, Sustain. Mater. Technol. 40 (July 2024) e00934.
[24] K. Scrivener, F. Martirena, S. Bishnoi, S. Maity, Calcined clay limestone cements (LC3), Cem. Concr. Res. 114 (Dec. 2018) 49–56.
[25] M. Antoni, J. Rossen, F. Martirena, K. Scrivener, Cement substitution by a combination of metakaolin and limestone, Cem. Concr. Res. 42 (Dec. 2012) 1579–1589.
[26] M. Sharma, S. Bishnoi, F. Martirena, K. Scrivener, Limestone calcined clay cement and concrete: a state-of-the-art review, Cem. Concr. Res. 149 (Nov. 2021) 106564.
[27] Y. Dhandapani, T. Sakthivel, M. Santhanam, R. Gettu, R.G. Pillai, Mechanical properties and durability performance of concretes with limestone calcined clay cement (LC3), Cem. Concr. Res. 107 (May 2018) 136–151.
[28] M. Beigh, V.N. Nerella, E. Secrieru, V. Mechtcherine, Structural build-up behavior of limestone calcined clay cement (LC^3) pastes in the context of digital concrete construction, in: 2nd International Conference on Rheology and Processing of Construction Materials (RheoCon2), Rheology and Processing of Construction Materials, Sept. 2019.
[29] T.R. Muzenda, P. Hou, S. Kawashima, T. Sui, X. Cheng, The role of limestone and calcined clay on the rheological properties of LC3, Cem. Concr. Compos. 107 (Mar. 2020) 103516.
[30] Li Chen, Chaves Figueiredo, Veer Çopuroğlu, Schlangen, Limestone and Calcined Clay-Based Sustainable Cementitious Materials for 3D Concrete Printing: A Fundamental Study of Extrudability and Early-Age Strength Development, Appl. Sci. 9 (Apr. 2019) 1809.
[31] M.A.B. Beigh, V.N. Nerella, C. Schröfl, V. Mechtcherine, Studying the Rheological Behavior of Limestone Calcined Clay Cement (LC3) Mixtures in the Context of Extrusion-Based 3D-Printing, in: S. Bishnoi (Ed.), Calcined Clays for Sustainable Concrete, Springer, 2020, pp. 229–236. RILEM Bookseries, (Singapore).
[32] W.-J. Long, C. Lin, J.-L. Tao, T.-H. Ye, Y. Fang, Printability and particle packing of 3D-printable limestone calcined clay cement composites, Constr. Build. Mater. 282 (May 2021) 122647.
[33] Y. Chen, S. He, Y. Zhang, Z. Wan, O. Çopuroğlu, E. Schlangen, 3D printing of calcined clay-limestone-based cementitious materials, Cem. Concr. Res. 149 (Nov. 2021) 106553.
[34] J. Yu, H.-L. Wu, D.K. Mishra, G. Li, C.K. Leung, Compressive strength and environmental impact of sustainable blended cement with high-dosage limestone and calcined clay (LC2), J. Clean. Prod. 278 (Jan. 2021) 123616.
[35] K.A. Ibrahim, G.P.A.G. van Zijl, A.J. Babafemi, Influence of limestone calcined clay cement on properties of 3D printed concrete for sustainable construction, J. Build. Eng. 69 (June 2023) 106186.
[36] Y. Gao, Y. Jiang, Y. Tao, P. Shen, C.S. Poon, Accelerated carbonation of recycled concrete aggregate in semi-wet environments: a promising technique for CO2 utilization, Cem. Concr. Res. 180 (June 2024) 107486.
[37] X. He, J. Zeng, J. Yang, Y. Su, Y. Wang, Z. Jin, Z. Zheng, C. Tian, Wet grinding carbonation technique: achieving rapid carbon mineralization of concrete slurry waste under low CO2 flow rate, Chem. Eng. J. 493 (Aug. 2024) 152836.
[38] S. Sánchez Berriel, A. Favier, E. Rosa Domínguez, I.R. Sánchez Machado, U. Heierli, K. Scrivener, F. Martirena Hernández, G. Habert, Assessing the environmental and economic potential of limestone calcined clay cement in Cuba, J. Clean. Prod. 124 (June 2016) 361–369.
[39] R. Gettu, A. Patel, V. Rathi, S. Prakasan, A.S. Basavaraj, S. Palaniappan, S. Maity, Influence of supplementary cementitious materials on the sustainability parameters of cements and concretes in the Indian context, Mater. Struct. 52 (Feb. 2019) 10.
[40] Z. Huang, W. Deng, X. Zhao, Y. Zhou, F. Xing, P. Hou, C. Chen, Shear design and life cycle assessment of novel limestone calcined clay cement reinforced concrete beams, Struct. Concr. 24 (4) (2023) 5063–5085. _eprint: https://onlinelibrary.wiley.com/doi/pdf/10.1002/suco.202200909.
[41] V. Sergis, C.M. Ouellet-Plamondon, Automating mix design for 3D concrete printing using optimization methods, Dig, Dis 1 (2022) 645–657, 10.1039.D2DD00040G.
[42] M. Finkbeiner, A. Inaba, R. Tan, K. Christiansen, H.-J. Klüppel, The new international standards for life cycle assessment: ISO 14040 and ISO 14044, Int. J. Life Cycle Assess. 11 (Mar. 2006) 80–85.
[43] NF EN 15804+A2, 2019.
[44] J.J. Chen, P.L. Ng, S.H. Chu, G.X. Guan, A.K.H. Kwan, Ternary blending with metakaolin and silica fume to improve packing density and performance of binder paste, Constr. Build. Mater. 252 (Aug. 2020) 119031.
[45] R. Gettu, A.S. Basavaraj, Life Cycle Assessment of LC3: Parameters and Prognoses, in: S. Bishnoi (Ed.), Calcined Clays for Sustainable Concrete, Springer, 2020, pp. 277–281. RILEM Bookseries, (Singapore).
[46] C. ASTM, Standard test method for flow of hydraulic cement mortar, in: C1437, 2007.
[47] C. ASTM, 143/C143M: standard test method for slump of hydraulic-cement concrete, Ann. Book ASTM Standar. 4 (2010) 89–91.
[48] N. Roussel, P. Coussot, et al., J. Rheol. 49 (May 2005) 705–718. Publisher: The Society of Rheology.
[49] D. ASTM, Standard Test Method for Direct Shear test of Soils Under Consolidated Drained Conditions, D3080/D3080M 3, 2011, p. 9.
[50] V. Sergis, C. Ouellet-Plamondon, D-optimal design of experiments applied to 3D high-performance concrete printing mix design, Mater. Des. 218 (Apr. 2022) 110681.
[51] R. Wolfs, F. Bos, T. Salet, Early age mechanical behaviour of 3D printed concrete: numerical modelling and experimental testing, Cem. Concr. Res. 106 (Apr. 2018) 103–116.
[52] ASTM, Standard Test Method for Compressive Strength of Hydraulic Cement Mortars (Using 2-in. Or [50-Mm] Cube Specimens), ASTM International, 2013.
[53] C. Mutel, Brightway: an open source framework for life cycle assessment, J. Open Sourc. Softw. 2 (Apr. 2017) 236.
[54] B. Steubing, D. de Koning, A. Haas, C.L. Mutel, The activity browser — an open source LCA software building on top of the brightway framework, Software Impact. 3 (Feb. 2020) 100012.
[55] R. Frischknecht, G. Rebitzer, The ecoinvent database system: a comprehensive web-based LCA database, J. Clean. Prod. 13 (Nov. 2005) 1337–1343.
[56] E. Saouter, F. Biganzoli, L. Ceriani, D. Versteeg, E. Crenna, L. Zampori, S. Sala, R. Pant, Environmental Footprint: Update of Life Cycle Impact Assessment Methods – Ecotoxicity Freshwater, human Toxicity Cancer, and Non-Cancer, Publications Office of the European Union, Jan. 2019 (ISBN: 9789276171430 9789276171423).
[57] M.A.J. Huijbregts, Z.J.N. Steinmann, P.M.F. Elshout, G. Stam, F. Verones, M. Vieira, M. Zijp, A. Hollander, R. van Zelm, ReCiPe2016: a harmonised life cycle impact assessment method at midpoint and endpoint level, Int. J. Life Cycle Assess. 22 (Feb. 2017) 138–147.
[58] J. Logan, C. Marcy, J. McCall, F. Flores-Espino, A. Bloom, J. Aabakken, W. Cole, T. Jenkin, G. Porro, C. Liu, F. Ganda, R. Boardman, T. Tarka, J. Brewer, T. Schultz, Electricity Generation Baseline Report, Tech. Rep. NREL/TP–6A20-67645, 1342379,, National Renewable Energy Laboratory, Jan. 2017.
[59] N. O. a. A. Administration, Distances Between United States Ports, 2019.
[60] Energy Statistics Data Browser – Data Tools, 2024.

[61] E.S. Arruda Junior, N.T. de Sales Braga, M.S. Barata, Life cycle assessment to produce LC^3 cements with kaolinitic waste from the Amazon region, Brazil, Case Stud. Constr. Mater. 18 (July 2023) e01729.
[62] Y. Cancio Díaz, S. Sánchez Berriel, U. Heierli, A.R. Favier, I.R. Sánchez Machado, K. L. Scrivener, J.F. Martirena Hernández, G. Habert, Limestone calcined clay cement as a low-carbon solution to meet expanding cement demand in emerging economies, Developm. Eng. 2 (Jan. 2017) 82–91.
[63] X. Qian, Y. Ruan, T. Jamil, C. Hu, F. Wang, S. Hu, Y. Liu, Sustainable cementitious material with ultra-high content partially calcined limestone-calcined clay, Constr. Build. Mater. 373 (Apr. 2023) 130891.
[64] X. Qian, X. Zhou, C. Hu, F. Wang, S. Hu, Role of partial limestone calcination in carbonated lime-based binders, Cem. Concr. Res. 183 (Sept. 2024) 107572.
[65] S. Bhattacherjee, S. Jain, M. Santhanam, Developing 3D printable and buildable limestone calcined clay-based cement composites with higher aggregate content, Constr. Build. Mater. 376 (May 2023) 131058.
[66] G. Habert, C. Ouellet-Plamondon, Recent update on the environmental impact of geopolymers, RILEM Techn. Lett. 1 (Apr. 2016) 17.
[67] A. Heath, K. Paine, M. McManus, Minimising the global warming potential of clay based geopolymers, J. Clean. Prod. 78 (Sept. 2014) 75–83.
[68] K.L. Scrivener, V.M. John, E.M. Gartner, Eco-efficient cements: potential economically viable solutions for a low-CO2 cement-based materials industry, Cem. Concr. Res. 114 (Dec. 2018) 2–26.
[69] A. Ito, R. Wagai, Global distribution of clay-size minerals on land surface for biogeochemical and climatological studies, Sci. Data 4 (Aug. 2017) 170103. Number: 1 Publisher: Nature Publishing Group.
[70] H. Kodama, Clay minerals in canadian soils: their origin, distribution and alteration, Can. J. Soil Sci. 59 (Feb. 1979) 37–58.
[71] S. Krishnan, D. Gopala Rao, S. Bishnoi, Why Low-Grade Calcined Clays Are the Ideal for the Production of Limestone Calcined Clay Cement (LC3), in: S. Bishnoi (Ed.), Calcined Clays for Sustainable Concrete, Springer, 2020, pp. 125–130. RILEM Bookseries, (Singapore).
[72] T. Wangler, N. Roussel, F.P. Bos, T.A.M. Salet, R.J. Flatt, Digital concrete: a review, Cem. Concr. Res. 123 (Sept. 2019) 105780.